Measuring the reflection of aluminium in vacuum with ultraviolet light

Yannick Wishaupt

30 juni 2023

STUDENT NUMBER	12610348
COURSE	Report Bachelor Project Physics and Astronomy, size 15 EC
PERIOD	Conducted between 03-04-2023 and 30-06-2023
INSTITUTE	NIKHEF
FACULTIES	FEW/VU & FNWI/UvA
SUPERVISOR	Tina Pollmann
SECOND EXAMINER	Marcel Vreeswijk

VU VRIJE UNIVERSITEIT AMSTERDAM | UNIVERSITEIT VAN AMSTERDAM

Abstract

The Deep Underground Neutrino Experiment (DUNE) is an upcoming experiment that focuses on detecting neutrinos and measuring their characteristics. DUNE consists of a modular liquid argon time-projection chamber (LArTPC), which is made of a significant amount of aluminium. Because DUNE uses the scintillation light of argon for their measurements, it is necessary to understand how aluminium reacts with UV- and VUV-light in order to improve our knowledge of the DUNE experiment. In this paper, I measure the reflectivity of aluminium with the Vacuum Ultraviolet Light Characterisation At Nikhef (VULCAN) setup to gain a better understanding of the optical properties of aluminium in the DUNE experiment. In our setup, a deuterium lamp creates a UV-light spectrum where a specific wavelength can be selected with a grating. Wavelengths from 120 to 200 nm are used to measure the reflectivity of an aluminium sample and a Silicon Photon Multiplier (SiPM) measures the intensity of the light. The intensity spectrum of the light hitting the sample is calculated by correcting a transmission measurement (I_0) for the different efficiency spectra of the components in the setup. The results show that ~ 47% of the light gets reflected at 200 nm and this decreases to ~ 14% at 120 nm. To improve this experiment, the intensity spectrum of the light hitting the sample should be measured for different wavelengths instead of calculated based on one I_0 measurement.

Populair wetenschappelijke samenvatting

Als we inzoomen tot de kleinste deeltjes van ons Universum, komen we tot de bouwstenen van ons Universum. Alle materie die we kunnen zien is hiervan gemaakt. We noemen deze deeltjes 'elementaire deeltjes' en zijn de fundamentele grondleggers van onze natuurkunde. Neutrino's zijn van dit soort deeltjes en kunnen worden gezien als ongeladen elektronen. Omdat neutrino's behoren tot de bouwstenen van ons Universum, is het erg belangrijk om te begrijpen hoe deze deeltjes werken. Ondanks dat alleen al de zon ongeveer 65 miljard elektron-neutrino's per seconde door je duim straalt, is het extreem moeilijk om neutrino's te detecteren omdat ze bijna niet met materie reageren. Inmiddels zijn er verscheidene experimenten die zich focussen op het detecteren van neutrino's, waaronder het 'Deep Underground Neutrino Experiment (DUNE)'. Om nauwkeurige metingen te kunnen doen, is het van belang om te weten hoe licht reageert met de materialen die worden gebruikt door DUNE. Aluminium is een van de meest gebruikte materialen in DUNE dus het is van belang om te weten hoe dit reageert met licht. De laatste drie maanden heb ik mij bezig gehouden met het meten van de reflectiviteit van aluminium in een vacuüm voor licht in het UV-spectrum. Dit verslag gaat in op mijn gedane metingen en bespreekt de bruikbaarheid van de resultaten.

Contents

1 Introduction

1.1 Neutrinos

Neutrinos are particles that belong to the fundamental building blocks of our Universe. They are part of the lepton family in the elementary particles and are electrically neutral with a spin of $\frac{1}{2}$. Naturally they are created in various ways, such as nuclear reactions and radioactive decay, but they can also be created in particle accelerators that we built for gaining a better understanding of our fundamental physics [1].

The idea of the neutrino was proposed in 1930 by the physicist Wolfgang Pauli, who predicted that there had to be an extra particle to fulfill the conservation laws in beta (β) decay [2]. Before this statement, physicists could not explain why certain nuclear reactions did not conserve energy and momentum. Pauli predicted that this hypothetical particle had to be electrically neutral and (almost) massless. He also stated that it would be hard to detect this particle as it would only interact with matter via the weakly interacting force.

In 1956, the first neutrino was detected by Clyde Cowan and Frederick Reines [3]. They did an experiment where they tried to create an inverse β-decay reaction, creating a neutron and a positron by the annihilation of an antineutrino and a proton:

$$\bar{\nu}_e + p \rightarrow n + e^+ \tag{1}$$

The positron would then annihilate with an electron, creating two gamma (γ) rays:

$$e^+ + e^- \rightarrow \gamma + \gamma \tag{2}$$

When Cowan and Reines succeeded in measuring this reaction, the first evidence of the existence of neutrinos was provided.

After the first detection, more techniques in measuring neutrinos followed. Raymond Davis Jr. was one of the first physicists to measure solar neutrinos and noticed that the amount of measured neutrinos was not in agreement with the predicted number [4]. This raised questions and Davis himself thought that there was something wrong with our understanding of the standard solar model. It was not until the early 2000s that the first evidence for oscillating neutrinos was provided [5]. According to this new theory, neutrinos could change their flavor (ν_e, ν_μ and ν_τ) while moving through space and this would explain why we could only see about $\frac{1}{3}$ of the amount of neutrinos produced by the sun. It also confirmed that neutrinos do have a small mass [6], which Pauli was not certain of.

After the discovery of neutrino oscillations, physicists had a better understanding in particle and nuclear physics. We now know that neutrinos are particles with a mass that can travel vast distances due to their weak interaction with matter. Neutrinos play therefore an important role in observing events such as supernovae and studying the early Universe.

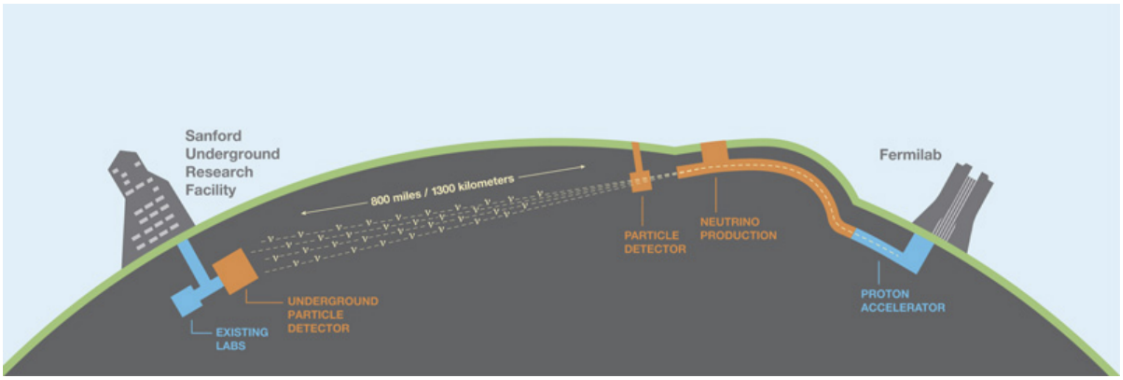

Figure 1: Schematic overview of the DUNE setup [7].

1.2 DUNE

There is a large number of experiments nowadays that focus on measuring neutrinos. One upcoming experiment is called the Deep Underground Neutrino Experiment (DUNE) [7]. DUNE's main goal is measuring neutrino oscillations, searching for proton decay and measuring the ν_e flux from a core-collapse supernova within our galaxy. Besides these topics, they also do measurements on physics beyond the standard model (BSM), neutrino oscillation phenomena using atmospheric neutrinos, studies of nuclear effects and searches for dark matter.

The DUNE experiment consists of a precision near detector located 575 m away from the Fermilab and a large, far detector about 1.5 km underground at the Sanford Underground Research Facility (SURF) (see Figure 1). At the Fermilab, protons get accelerated and produce an intense beam of neutrinos. This beam then gets directed to the far detector which is a large, modular liquid argon time-projection chamber (LArTPC). The far detector at SURF makes it possible to detect and measure neutrino interactions, while the near detector at the Fermilab can measure the intensity and energy spectrum of the wide-band beam of neutrinos with a high accuracy. These two detectors combined provide the ability to measure the properties of neutrinos in their different flavours.

1.3 Project outline

For the last three months I have been working with Vacuum Ultraviolet Light Characterisation At Nikhef (VULCAN). Their goal is to gain a better understanding of the optical properties of materials for scintillation based time projection chambers (TPCs). The most used material in DUNE's TPCs is aluminium, so it is necessary to gain a better understanding of how aluminium reacts within the VULCAN-setup. My part in this experiment is to measure the reflectivity of aluminium with UV-light inside a vacuum to improve our knowledge of the DUNE experiment.

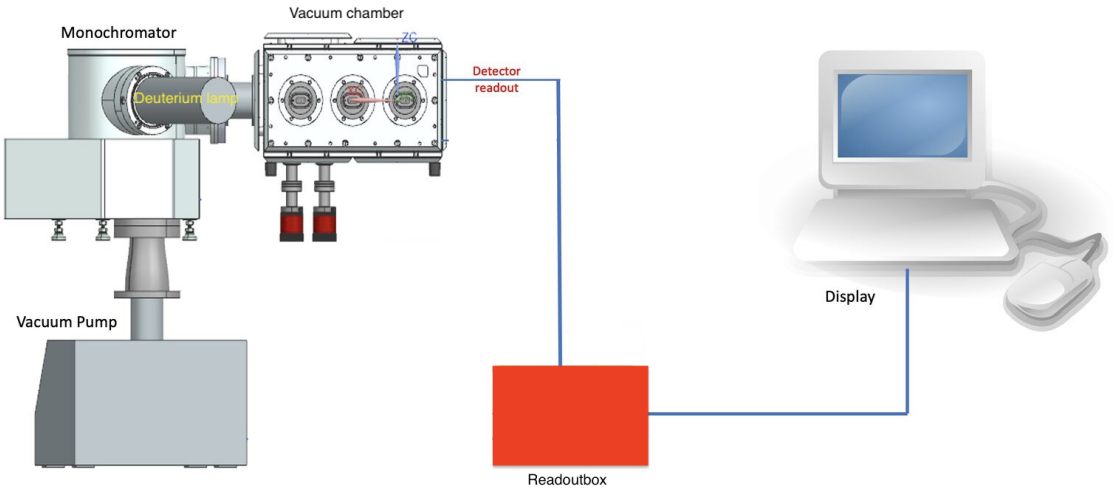

Figure 2: Schematic overview of the VULCAN-setup.

2 VULCAN-setup

The VULCAN-setup consists of several components (see Figure 2):

- Hamamatsu deuterium lamp
- McPherson Monochromator
- Pfeiffer vacuum pump
- Vacuum chamber
- Sample holder
- SiPMs
- Amplifier
- Data acquisition system

2.1 Deuterium lamp and monochromator

In the VULCAN-setup, we use a deuterium lamp to create a light beam that covers the VUV- and UV-spectra (see Figure 3). The lamp is filled with deuterium gas that gets excited and ionized by an applied electric field. When the ionized atoms return to their lower energy states, photons in the VUV- and UV-regions are emitted and get sent to the monochromator.

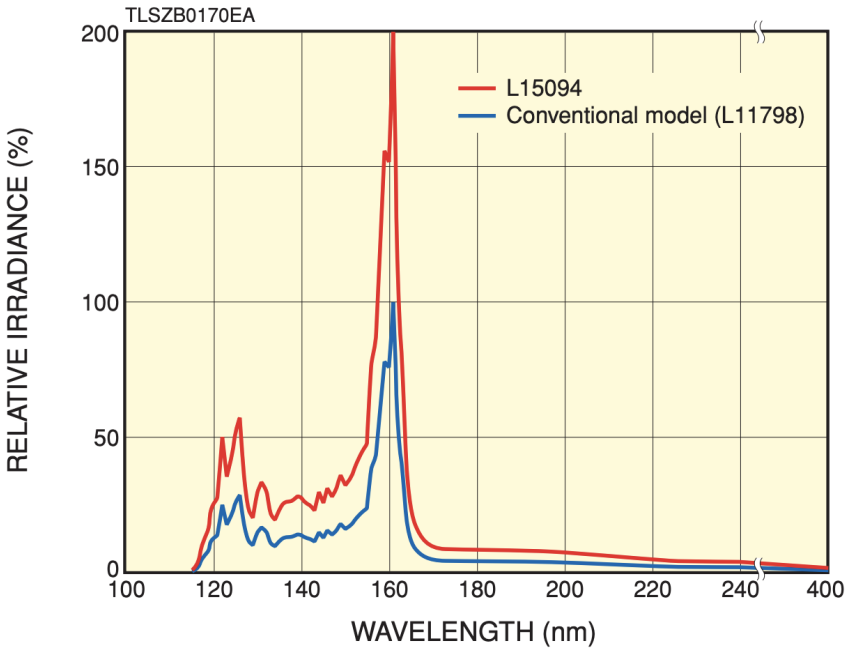

Figure 3: The blue line shows the intensity spectrum for different wavelengths of the deuterium lamp used in the VULCAN-setup, normalized to the peak at 160 nm [8].

The monochromator consists of a vacuum chamber, an entrance slit, a grating (2.2) and an exit slit. With the entrance slit, the intensity of the light going into the monochromator can be adjusted. The exit slit can narrow and widen the outgoing beam that hits the sample.

2.2 Grating

The grating inside the monochromator selects a specific wavelength out of a wide spectrum of light. It consists of parallel placed grooves that cause the light to diffract in different wavelengths due to constructive and destructive interference (see Figure 4). One can select a specific wavelength by changing the angle of the grooves relative to the incoming light beam according to

$$m\lambda = d \cdot \sin(\theta) \tag{3}$$

where m is the order of diffraction, λ the wavelength, d the distance between the grooves and θ the angle of incidence. For this experiment a 1200

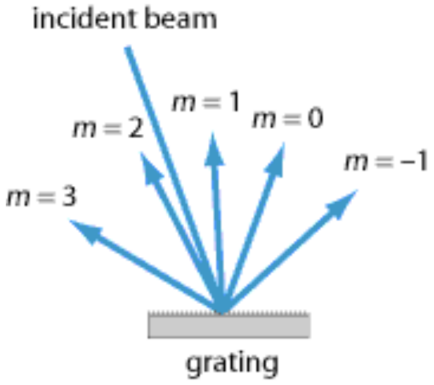

Figure 4: Schematic overview of how a grating works [9].

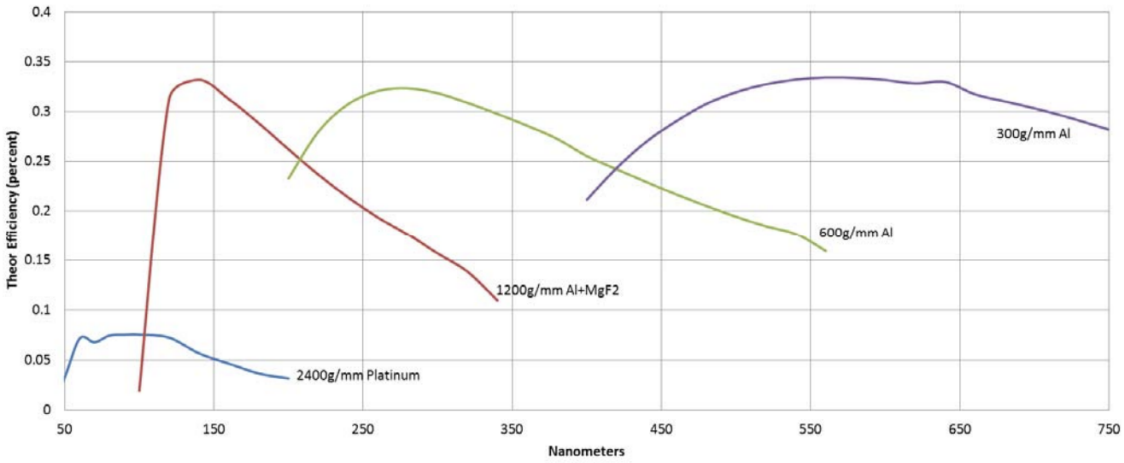

Figure 5: The red line shows the efficiency of the grating used in the VULCAN-setup at different wavelengths [10].

g/mm Al+MgF2 grating is used, so

$$d = \frac{1}{1200} \cdot 10^{-3} = 8.3 \cdot 10^{-7} \text{ m} \tag{4}$$

The 0^{th} order wavelength is then directed towards the exit slit of the monochromator and enters the vacuum chamber. Figure 5 shows the spectrum of the efficiency of the grating at different wavelengths.

2.3 Vacuum pump and chamber

UV-light gets easily absorbed by oxygen (see Figure 6). It is therefore necessary to do measurements inside a vacuum. To create a vacuum, we use a vacuum chamber made by IdealVac and a vacuum pump made by Pfeiffer. The pressure can go down to the order of 10^{-5} mbar, which is sufficient for the measurements as the absorption of UV-light by oxygen drops down to below 0.01% at that pressure.

A sample holder that will hold the aluminium sample is placed inside the vacuum chamber. Figure 7 shows how this looks like from the inside. The sample holder is made of copper and has two sides where a sample can be placed. Cooling braids can be attached to the sample holder to cool the sample, but this feature was not yet available in this experiment. With two rotating arms, the sample- and sensor holder can be rotated from outside the vacuum chamber.

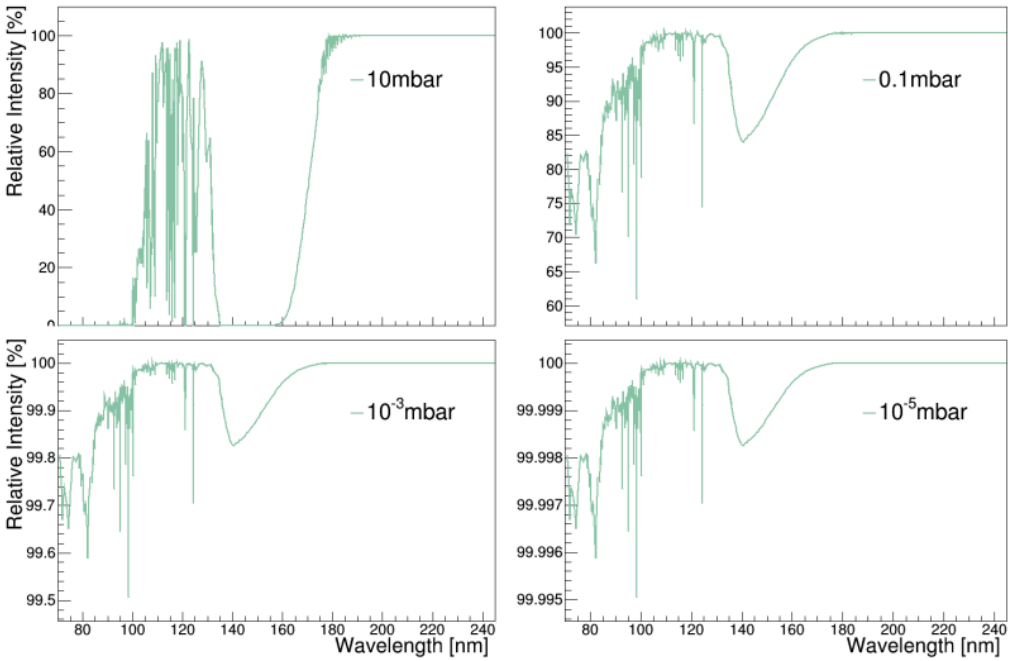

Figure 6: Relative intensity spectrum of UV-light at different pressures at 0.3 m [11].

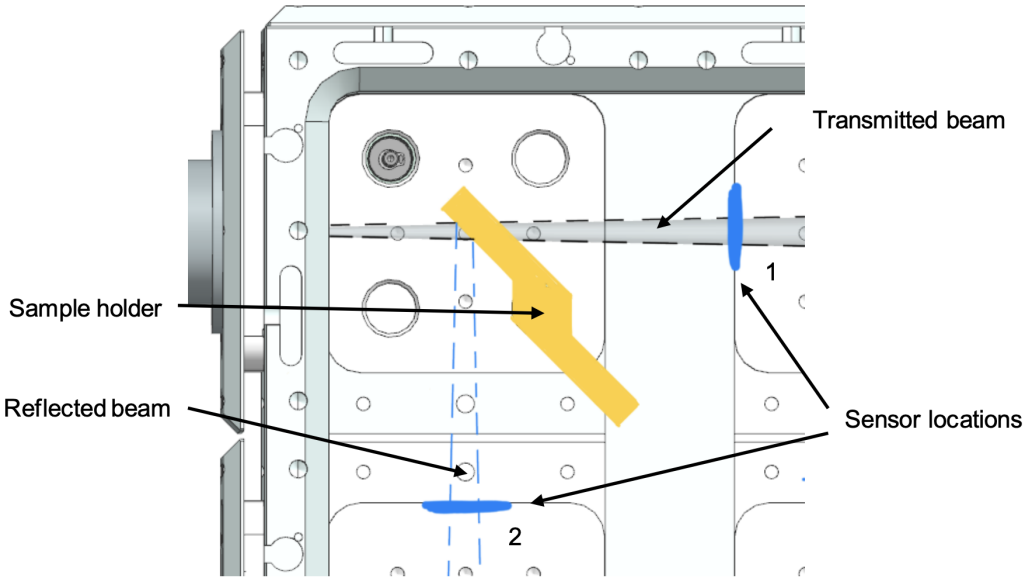

Figure 7: Schematic overview from the inside of the vacuum chamber [12].

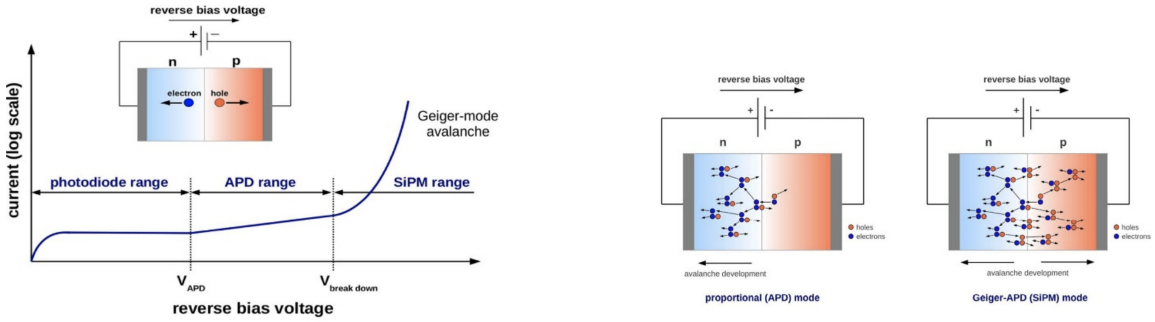

(a) Different stages of a SPAD.

(b) Avalanche process of a SPAD.

Figure 8: Schematic overview of how a SPAD works [13].

2.4 SiPM

For measuring the photons inside the vacuum chamber, Silicon Photon Multipliers (SiPMs) are used [13]. A SiPM consists of an array of thousands of single-photon avalanche diodes (SPADs) where each SPAD is able to detect a singe photon. This makes it possible for SiPMs to detect the amount of incoming photons with high precision.

A SPAD is a semiconductor that operates as a reverse-biased p-n junction. This means that the negatively charged side of the diode is attached to a higher voltage then the positively charged side (see 8a). When a photon hits the diode, an electron-hole pair is created and an electric current proportional to the energy of the photon will flow due to the applied electric field. When one increases the bias voltage to above the breakdown voltage ($V_{\text{breakdown}}$), the electron-hole pair generates enough kinetic energy to create more electron-hole pairs. We call this the avalanche development and can be seen in Figure 8b. When this happens, an electric current can be measured and thus a photon has been detected. To stop the avalanche process, a quenching circuit brings the bias voltage to or below $V_{\text{breakdown}}$. The voltage then gets restored after tens to hundreds of nanoseconds (depending on the SiPM design) so that the SPAD is operating again.

The thermal generation frequency of the SiPMs depends on the temperature, which means that SiPMs measure more noise at higher temperatures. We call these measurements dark-counts, as they are not generated by photons. In order to compensate for these darkcounts, one has to do a measurement without any light and subtract this from the measurements done with light. In our setup we do not yet have a cooling mechanism, so a darkcount measurement is necessary.

In the VULCAN-setup, VUV-MPPC 4th generation (VUV4) SiPMs are used [14]. This model is used because it covers the scintillation wavelengths of liquid xenon and argon, mak-

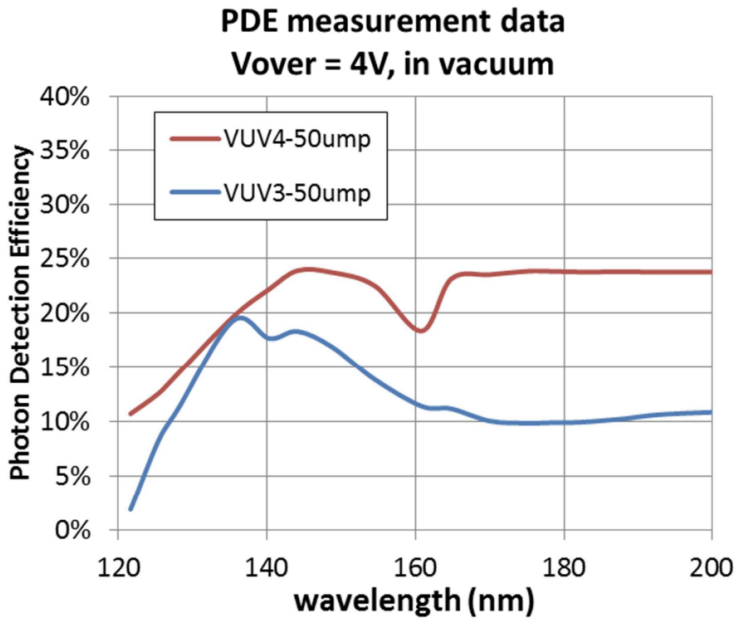

Figure 9: The red line shows the SiPM efficiency for this setup at different wavelengths [14].

ing it suitable for dark matter and neutrino experiments. Figure 9 shows the efficiency of the SiPM for different wavelengths. We soldered conducting wires on the SiPMs so they can be used inside a vacuum.

2.5 Amplifier and data acquisition system

After a signal is sent by a SiPM, it gets amplified by an amplifier in order to get a readable output. This is then converted to binary code which we can read with a computer. To analyse the data, we can use two different methods to count the photons:

- integration method
- peak-finding method

The integration method calculates the amount of photons that have been detected by integrating the output of the SiPM. The peak-finding method identifies peaks and counts the number of detected peaks, which represents the amount of detected photons. The peak-finding method is precise in finding an event, but not precise in finding how much photons were detected in one single event as this method does not count the height of the peaks. The integration method however does find multiple photons at one event, but also includes more noise.

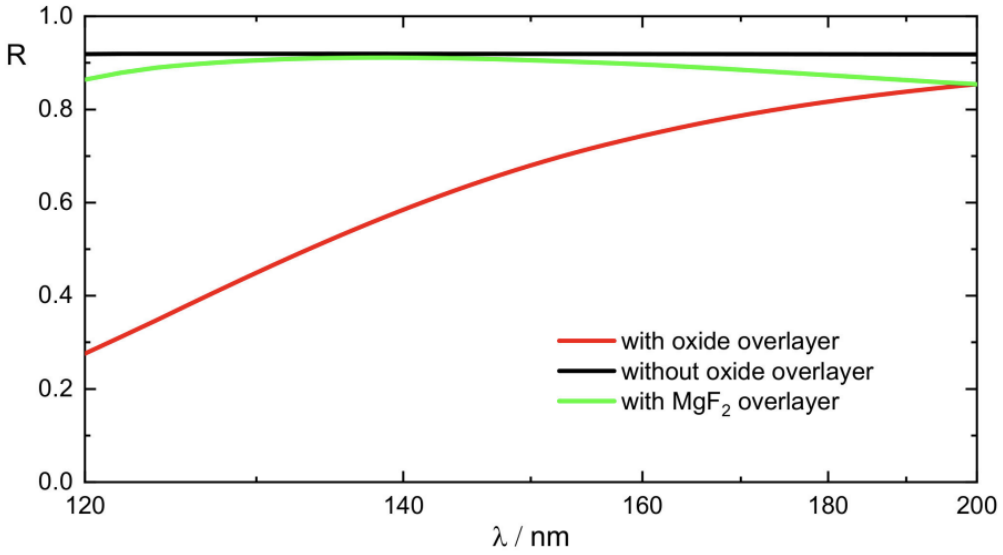

Figure 10: Reflectivity profile of aluminium for VUV-light, measured in a comparable experiment done by O. Stenzel [15].

3 Measuring the reflectivity of aluminium

3.1 Method

To measure the reflectivity of aluminium with the VULCAN-setup, we used an aluminium sample whose reflectivity profile was already measured by a comparable experiment done by O. Stenzel [15]. The red line in Figure 10 shows the predicted reflectivity spectrum for our experiment as our sample has been exposed to oxygen for a relatively long time.

For a single measurement, we saved 5000 data-sets of the output of the SiPM with an interval of ~ 13000 ns between each data-set for a specific wavelength. We did this inside a vacuum for wavelengths between 120 nm and 200 nm, increasing the wavelength with 5 nm after each measurement. The entrance slit was set on 0.04 mm and the exit slit was set on 2 mm. The breakdown voltage ($V_{\text{breakdown}}$) was ~ 55 V, so we set the bias voltage to 57 V.

The intensity spectrum of the light beam hitting the sample is different at different wavelengths due to the lamp spectrum (3), grating efficiency (5) and SiPM efficiency (9). In order to correct for these spectra, we measured an I_0, which was a transmission measurement at a wavelength of 180 nm (section 3.4 will explain this in more detail). The measured I_0 is then corrected for the lamp spectrum, grating efficiency and SiPM efficiency. After correcting I_0 for the desired wavelengths, we divided the measured reflectivity spectrum by this new found I_0^{corr} spectrum to get a relative intensity profile of the reflectivity of aluminium.

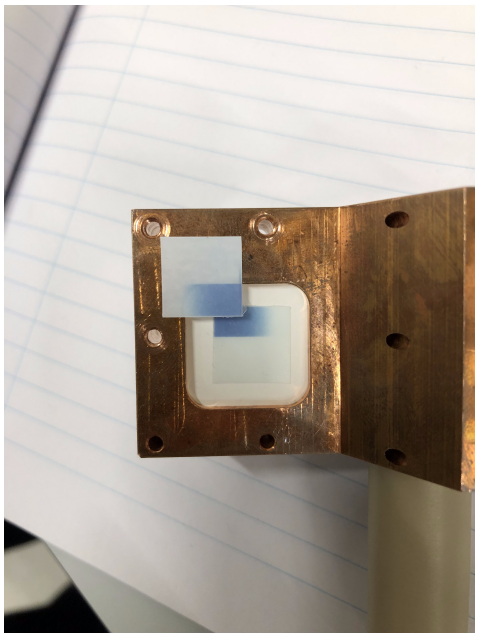

(a) Before adjustment.

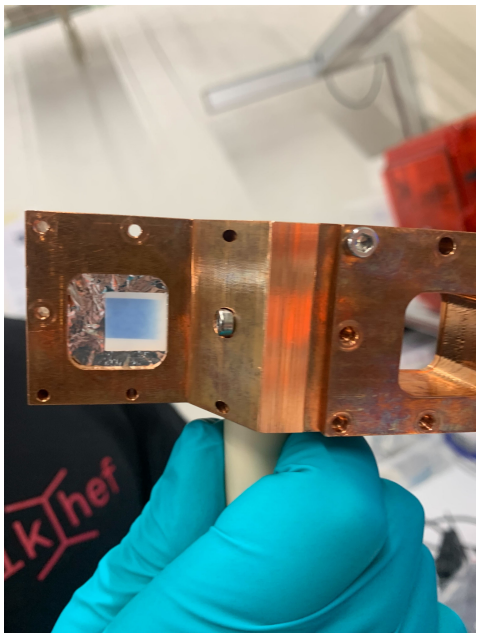

(b) After adjustment.

Figure 11: The UV-sensitive paper shows where the light beam hit the sample holder before and after the adjustment.

3.2 Correcting the sample holder

When we checked the alignment of the light beam hitting the sample holder [1], we noticed that the light did not hit the sample holder at the place we wanted it to hit. With UV-sensitive paper, we measured the offset of the alignment and concluded that the sample holder needed to be:

- 6 mm higher
- 3.5 mm wider each side (7 mm in total)

Once adjusted, the UV-light hit the sample window vertically in the middle and horizontally 1 mm from the right side of the sample window. This is necessary because the sample holder will be turned when measuring the reflectivity (see Figure 7). Figure 11 shows the final alignment versus the first alignment.

[1] When the wavelength of the monochromator is set at 0.0 nm, all the light of the lamp gets reflected and one is able to actually see the light beam hitting the sample holder.

3.3 Simulation of reflectivity measurement

I used Python code to predict the behavior of the light inside the vacuum chamber. I extended some code that was already available and I made some additional code for a 3D simulation.

In this report, we define a fully horizontally alignment of the sample- and sensor holder as 0° and a positive angle means turning the holders anti-clockwise. We turned the sample holder 37° to do the measurements (see Figure 12a). This angle was chosen because the 3D simulation showed that a higher angle results in a lower surface of the light beam hitting the SiPM (the blue dot in Figure 12b), but increasing the angle also means that the light beam hits the sample holder window closer to the edge. When choosing 37°, the beam still hits the sample fully and the surface of the light beam is relatively small.

Figure 12a shows the angles and distances of interest when turning the sampler holder 37°. To measure the reflectivity of this angle, the sensor holder needs to be turned 3.30°. The SiPM then makes an angle of 19.30° with the light beam. The total length of the path that the light travels is 159.44 mm. To measure I_0, the sensor holder needs to be turned 77.04°. The SiPM then makes an angle of 12.96° with the light beam and the light travels 145.69 mm before it hits the SiPM. The difference in distance between the reflection measurements and the I_0 measurement is 159.44 – 145.69 = 13.75 mm. The light beam diverges so the reflection measurements should measure a lower intensity than the I_0 measurement, but this difference is negligibly small.

3.4 Corrected intensity spectrum

As discussed in section 3.1, we need to correct the measured I_0 for the lamp, grating and SiPM. The uncertainty on these devices is set to ~ 10% each for this experiment. When we divide the measured reflectivity spectrum by the corrected I_0^{corr} spectrum, we get the reflectivity spectrum of aluminium in this setup. The error is then calculated based on the standard deviation of the measurements and on the uncertainty of the lamp, grating and SiPM.

The total correction spectrum we have to apply on I_0 is given by:

$$\mathrm{C}_{\text{total}} = \mathrm{C}_{\text{lamp}} \cdot \mathrm{C}_{\text{grating}} \cdot \mathrm{C}_{\text{sipm}} \tag{5}$$

where C stands for the correction (see Figure 13). The total correction spectrum for I_0 is then calculated by:

$$I_0^{\text{corr}} = \frac{I_0^{\text{meas}} \cdot \mathrm{C}_{\text{total}}}{\mathrm{C}_{180}} \tag{6}$$

where I_0^{meas} is the measured intensity of I_0 at 180 nm and C_{180} is the correction at 180 nm [2].

[2] We measured I_0 at a wavelength of 180 nm.

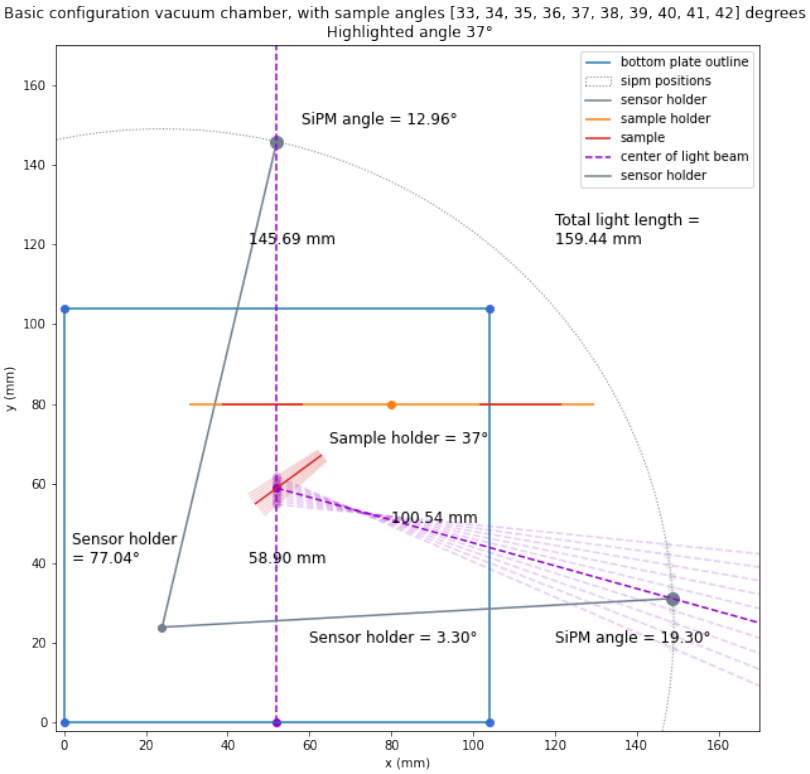

(a) 2D reflectivity simulation.

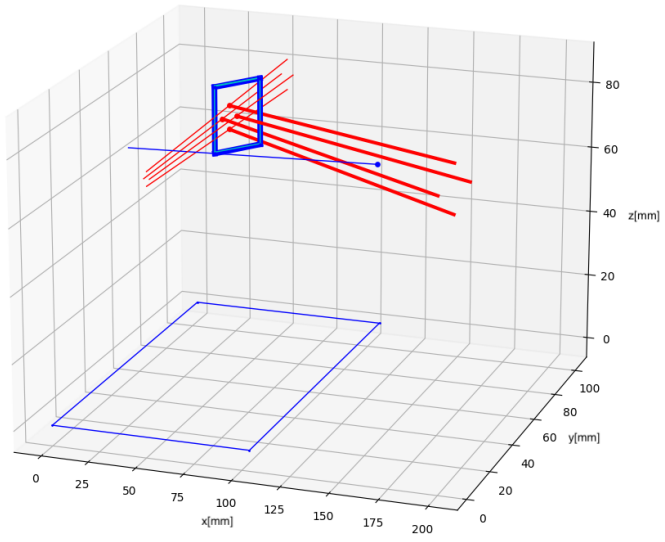

(b) 3D reflectivity simulation.

Figure 12: Simulation of the reflectivity profile in 2D and 3D.

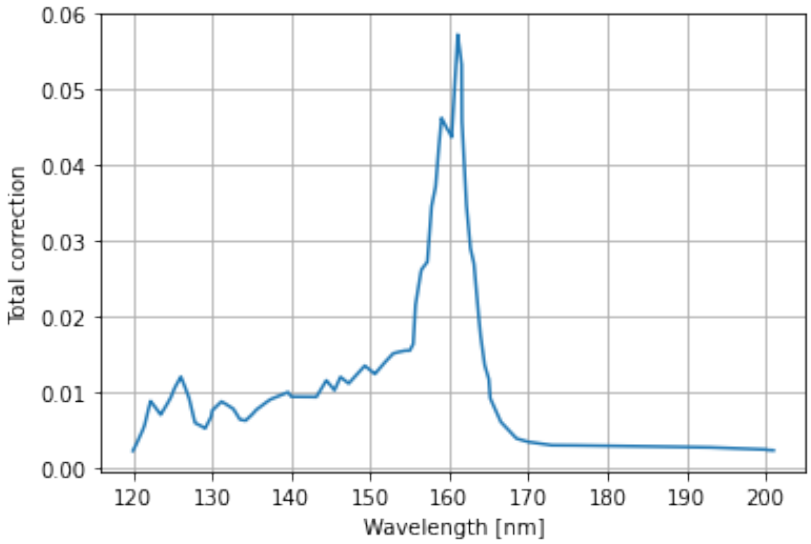

Figure 13: Total correction spectrum we need to apply to the measured I_0.

In order to correct for the angles of incidence of the light on the SiPM, we use the formula

$$I_{\theta=0} = \frac{I_\theta}{\cos(\theta)} \tag{7}$$

where $I_{\theta=0}$ is the intensity without an angle between the SiPM and the light beam, I_θ is the measured intensity of the SiPM with an angle of θ and θ is the angle of incidence of the light beam on the SiPM.

The final intensity spectrum of the reflectivity is then calculated by correcting the measured reflectivity spectrum with the corrected I_0^{corr} spectrum (6) and the angles of the SiPMs (7):

$$I_{\text{corr}} = \frac{\cos(\theta_{I0})}{\cos(\theta_{\text{meas}})} \cdot \frac{I_{\text{meas}}}{I_0^{\text{corr}}} \tag{8}$$

This spectrum can be compared with the predicted reflectivity spectrum of aluminium (10) and this will tell us more about the reliability and behavior of our setup.

4 Results

In order to do measurements inside a vacuum, we had to align the light beam with the sample holder before turning on the vacuum pump. We did so by setting the wavelength of the monochromator to the reflective setting (0.0 nm), after which we aligned the sensor-holder visually by turning the sensor-holder until the light beam hit the SiPM. As shown in Figure 12a, this corresponds to an angle of 77.04°. We then turned the sensor holder to 3.30° and aligned the sample holder visually by turning the sample-holder until the light beam hit the SiPM after reflection.

After the alignment, we turned on the pressure pump and waited until we got a pressure of $5.4 \cdot 10^{-4}$ mbar (see Figure 15). We then started our measurements with a darkcount, so without any light. A random single snapshot from the darkcount measurement can be seen in Figure 16a, where 16b shows the baseline correction of this snapshot.

After the darkcount, we did reflectivity measurements where the grating went from 120 to 200 nm, increasing the wavelength by 5 nm after each measurement. Figure 17 shows a random snapshot from a measurement at 180 nm.

Finally we did an I_0 measurement as described in section 3.1 at a wavelength of 180 nm. This could have been any other wavelength, as we know how the light behaves at all wavelengths according to 13.

After the measurements, I analyzed the results with the integration method as described in section 2.5. I subtracted the darkcounts from all the measurements, divided the remaining part by the calculated I_0^{corr} spectrum as described in equation 8 and plot the results (see Figure 14). At 200 nm, $\sim 47\%$ gets reflected and this decreases to $\sim 14\%$ at 120 nm.

5 Conclusion and discussion

The trend that the results show is expected (see Figure 10), but the experiment done by Stenzel showed that the intensity at 200 nm should be in the range of $\sim 85\%$ and this should decrease to $\sim 30\%$ at 120 nm.

For the experiment, we used an aluminium sample that did not have a perfectly flat and clean surface due to surface defects and oxidation. It was also a relatively old sample compared to the sample used by Stenzel. The reflection spectrum of this sample is therefore not expected to be exactly as the one shown in Figure 10. In order to improve the measurements and gain a better understanding of the reflectivity in the VULCAN-setup, one should consider using a sample where the reflectivity profile is known with high accuracy.

The temperature during the measurements was $\sim 21°$ C (see Figure 15). As discussed in section 2.4, a higher temperature increases the darkcounts which is something we want to reduce as much as possible. We did not yet have a cooling mechanism, so our darkcounts were relatively high. In a future experiment, the inside of the vacuum chamber and the sample holder need to be cooled down for more accurate results.

As discussed in section 3, measuring the reflectivity of aluminium was done by dividing the measured reflectivity spectrum by a calculated I_0^{corr} spectrum. This caused the error bars to enlarge for bigger wavelengths, because the intensity of the light drops rapidly for wavelengths above 160 nm (see Figure 13). This means that we have to correct for this value and its error with a relatively high factor, resulting in higher error bars. An improvement would be to

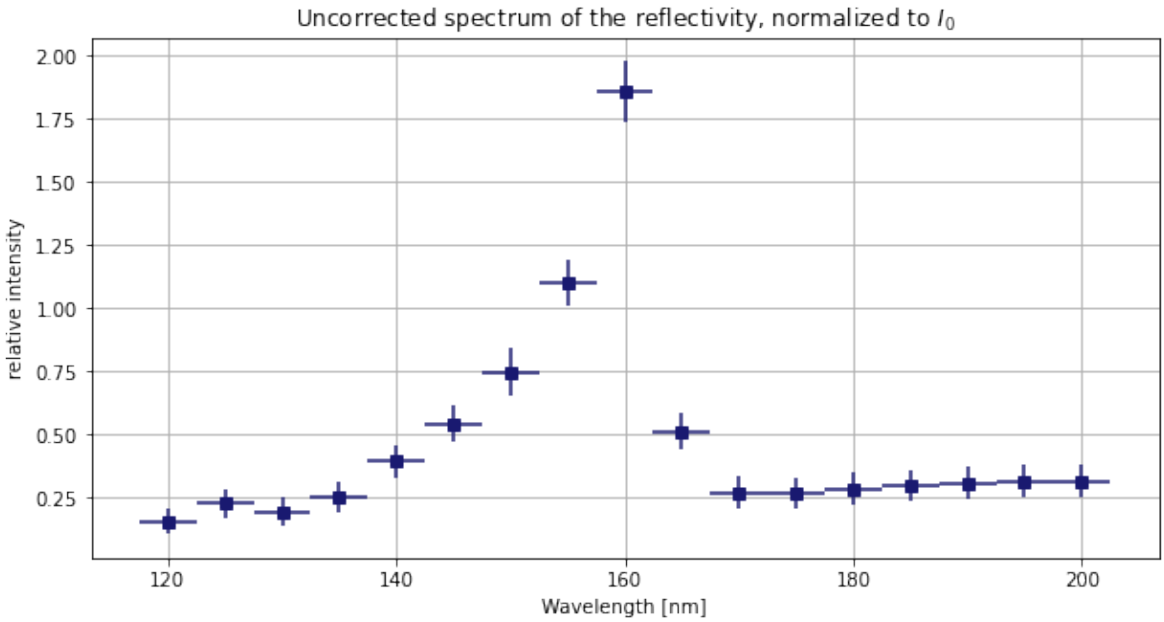

(a) Uncorrected reflectivity spectrum.

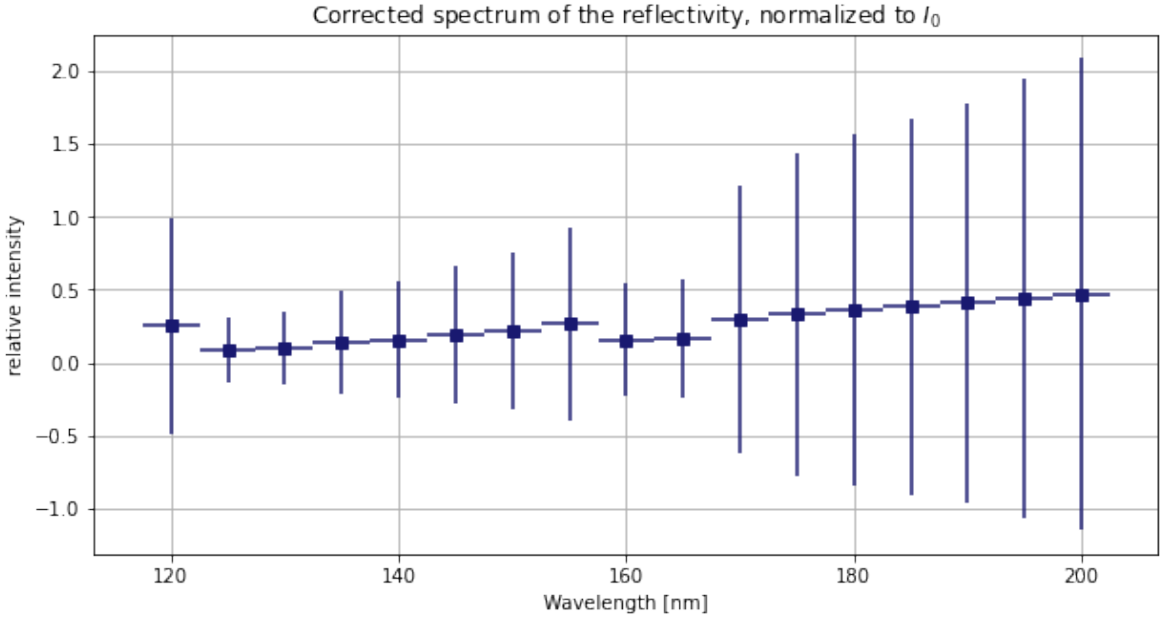

(b) Corrected reflectivity spectrum.

Figure 14: The measured reflectivity spectrum of aluminium in the VULCAN-setup.

measure I_0 at a wavelength with a higher intensity as this will probably give a more accurate I_0^{corr} spectrum.

The lamp, grating and SiPM are the cause of the large error bars as the uncertainty on these devices is set on $\sim 10\%$ each. When we remove these errors and assume that the error on these devices is 0%, we would get a result as shown in Figure 18. In the future it would be better to reduce the uncertainty of the components in the setup as this will give more accurate measurements.

To improve this experiment, I suggest to measure the intensity profile of the lamp at different wavelengths instead of calculating it by correcting a measured I_0 for all the correction spectra. This would avoid the uncertainties of the different components in the setup and give a more accurate intensity profile of the light beam with only the standard deviation as its error. After this measurement, one can measure the reflectivity of a sample and divide this spectrum by the measured intensity spectrum. This gives you a relative reflectivity spectrum for all wavelengths with a higher accuracy.

In summary, the measured reflectivity spectrum of the aluminium sample show a similar trend as the expected trend, but the exact values are not in agreement with the expected values. This is due to the uncertainties of the components in the VULCAN-setup and the fact that we do not know the reflectivity profile of the used sample with high accuracy. In order to gain a better understanding of the DUNE experiment, my experiment can be improved by measuring the intensity profile of the light beam for different wavelengths instead of calculating it, by using a sample whose reflectivity profile is know with a higher accuracy, and by reducing the temperature of the vacuum chamber to reduce the darkcounts.

Acknowledgements

I want to thank Tina Pollmann for having me and introducing me to the VULCAN-setup. It was fun to gain experience in experimental physics, even though I did not know in advance whether I would like it or not. It has been a pleasure to help the VULCAN group with their setup and I wish them all the best for future experiments.

Further more I want to thank Marjolein van Nuland and Vikas Gupta for their daily help and support. They gave me all the feedback I needed and thanks to them, I knew how I could contribute in an efficient way. Soon I hope that the setup will work as they want it to work and that the results will be as expected.

And last but not least, I want to thank the whole Dark Matter group for the last three months. I will miss the laughs we had during the lunch- and coffee-breaks, which made me have a fun time at Nikhef.

A Appendix of section 4

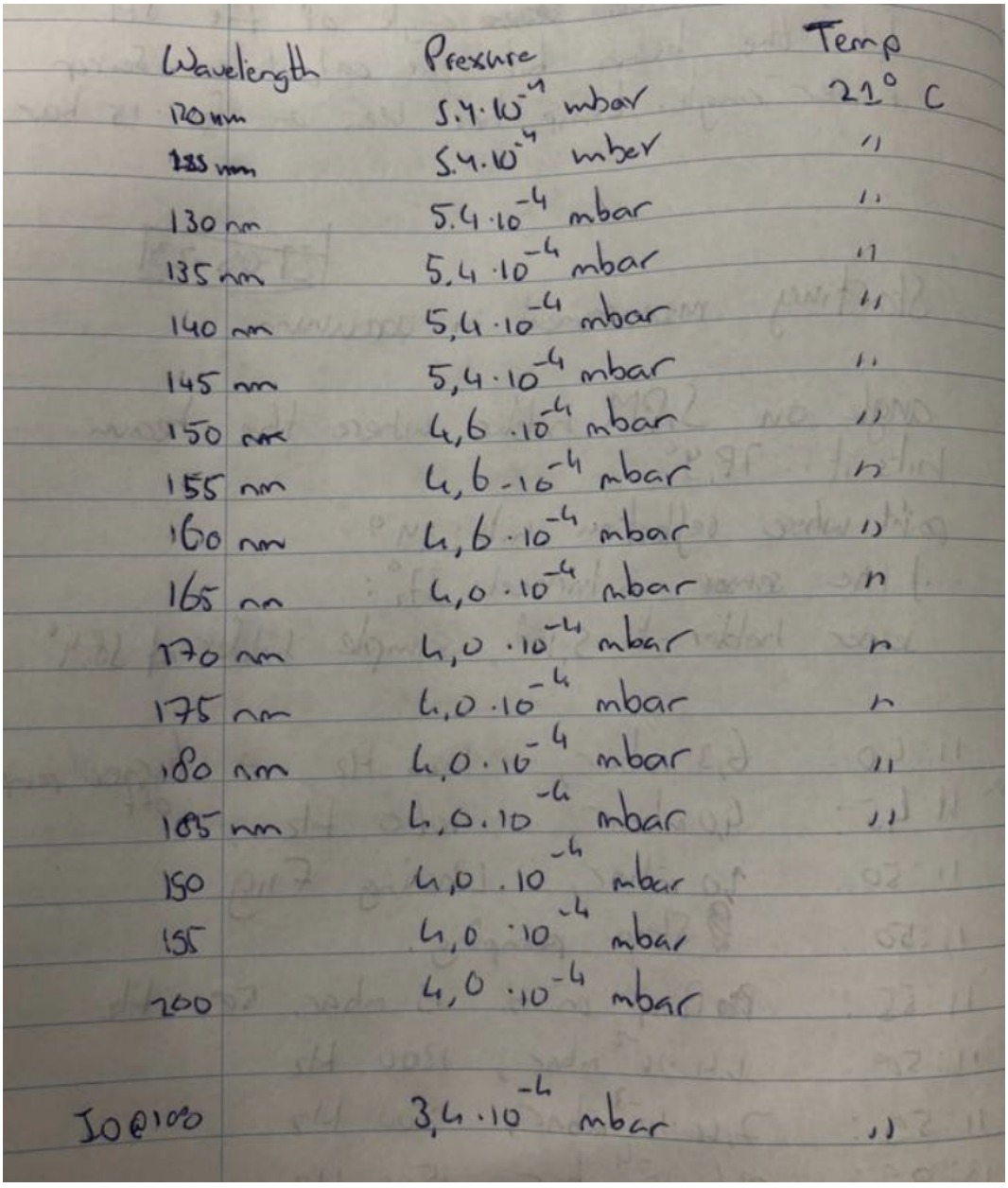

Wavelength	Pressure	Temp
120 nm	$5.4 \cdot 10^{-4}$ mbar	21° C
125 nm	$5.4 \cdot 10^{-4}$ mbar	"
130 nm	$5.4 \cdot 10^{-4}$ mbar	"
135 nm	$5,4 \cdot 10^{-4}$ mbar	"
140 nm	$5,4 \cdot 10^{-4}$ mbar	"
145 nm	$5,4 \cdot 10^{-4}$ mbar	"
150 nm	$4,6 \cdot 10^{-4}$ mbar	"
155 nm	$4,6 \cdot 10^{-4}$ mbar	"
160 nm	$4,6 \cdot 10^{-4}$ mbar	"
165 nm	$4,0 \cdot 10^{-4}$ mbar	"
170 nm	$4,0 \cdot 10^{-4}$ mbar	"
175 nm	$4,0 \cdot 10^{-4}$ mbar	"
180 nm	$4,0 \cdot 10^{-4}$ mbar	"
185 nm	$4,0 \cdot 10^{-4}$ mbar	"
190	$4,0 \cdot 10^{-4}$ mbar	
195	$4,0 \cdot 10^{-4}$ mbar	
200	$4,0 \cdot 10^{-4}$ mbar	
I0 @100	$3,4 \cdot 10^{-4}$ mbar	"

Figure 15: Measured pressure and temperature during the measurements.

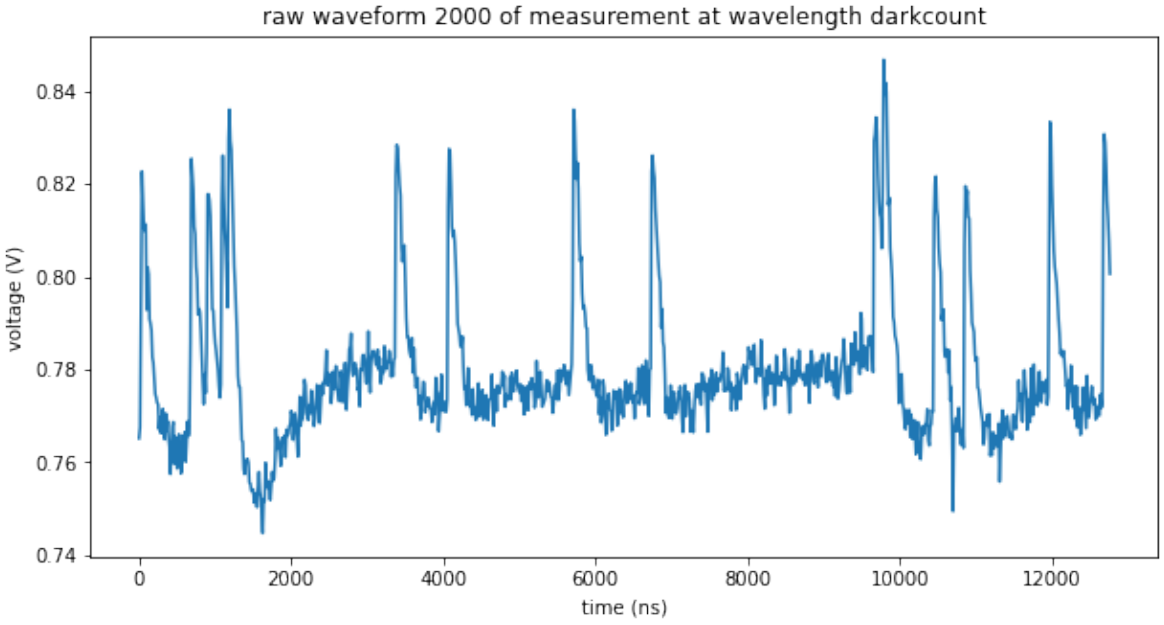

(a) Single snapshot of darkcount.

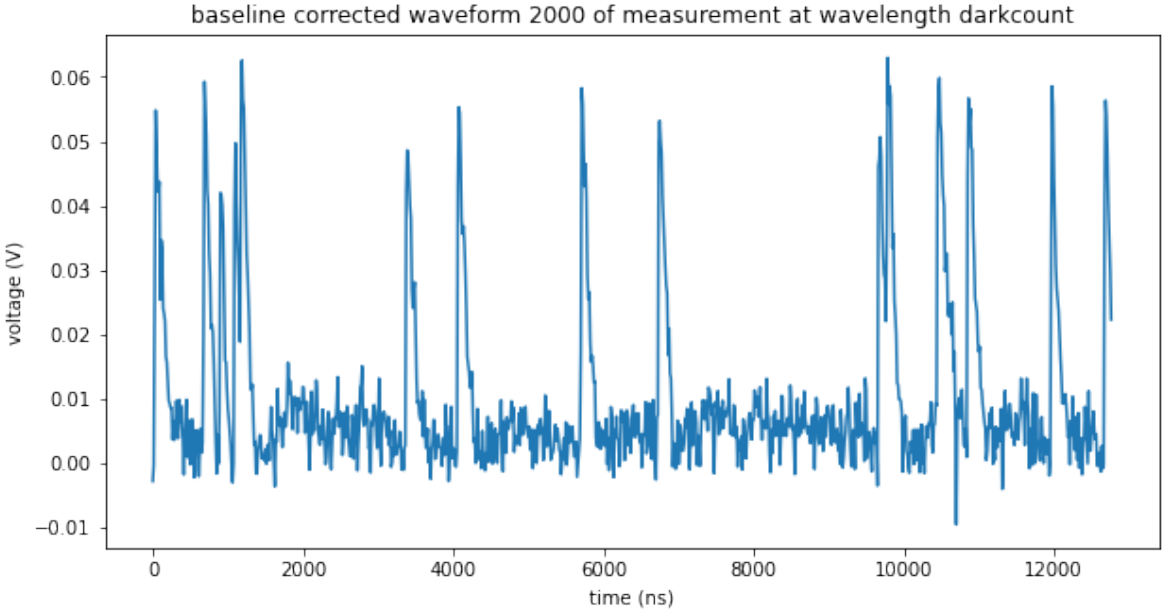

(b) Baseline corrected snapshot of darkcount.

Figure 16: Random snapshot from the darkcount measurement.

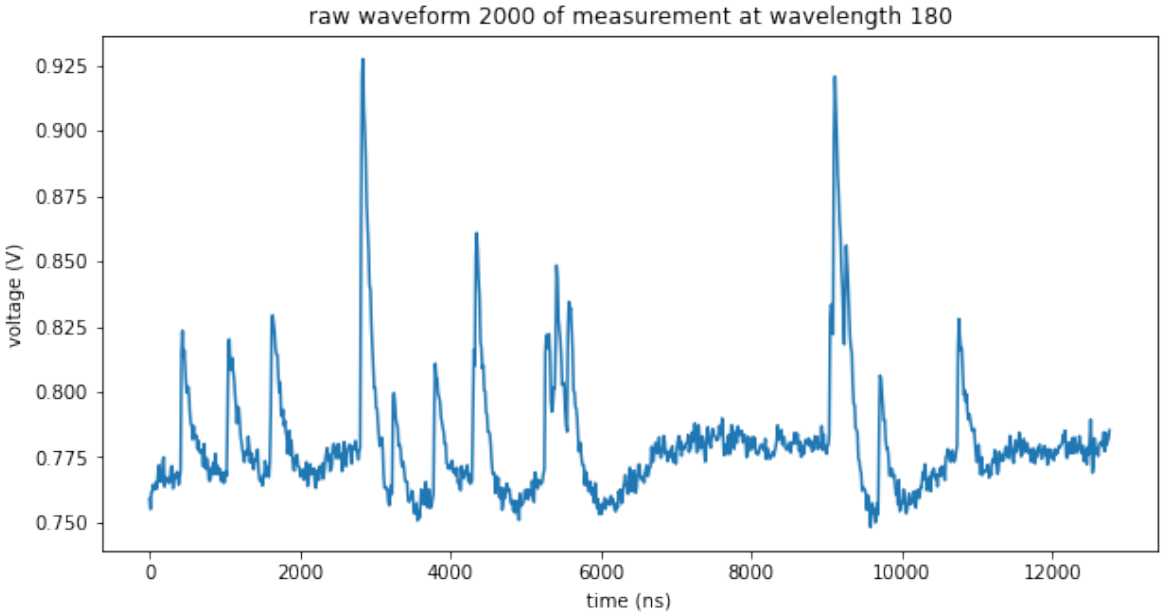

(a) Single snapshot of measurement at 180 nm.

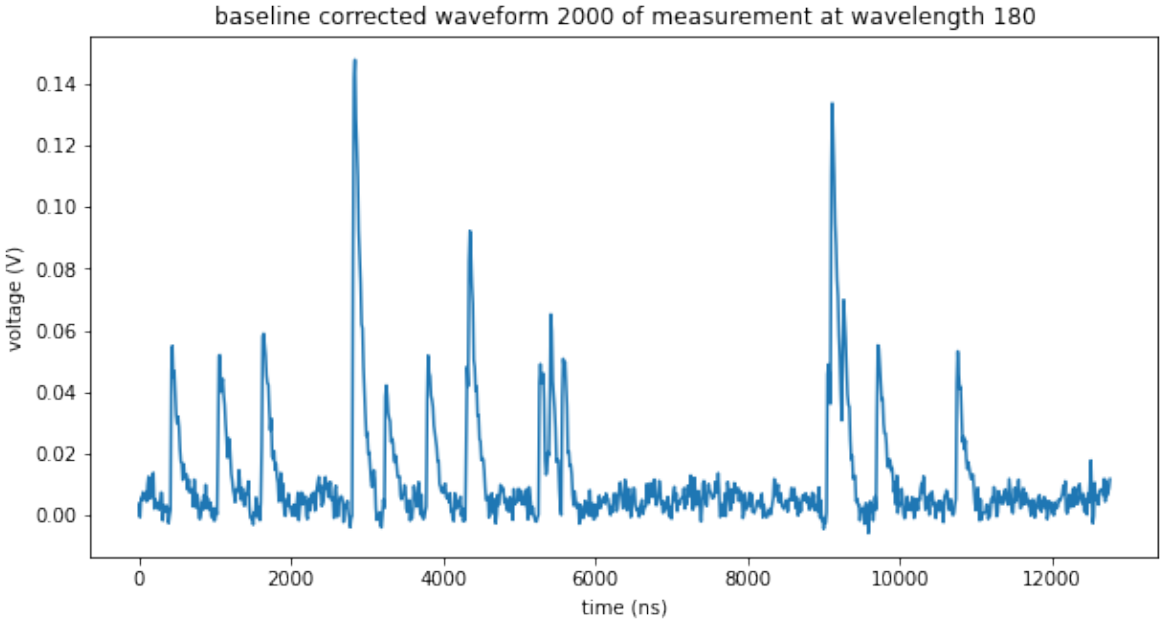

(b) Baseline corrected snapshot of measurement at 180 nm.

Figure 17: Random snapshot from measurement at 180 nm.

B Appendix of section 5

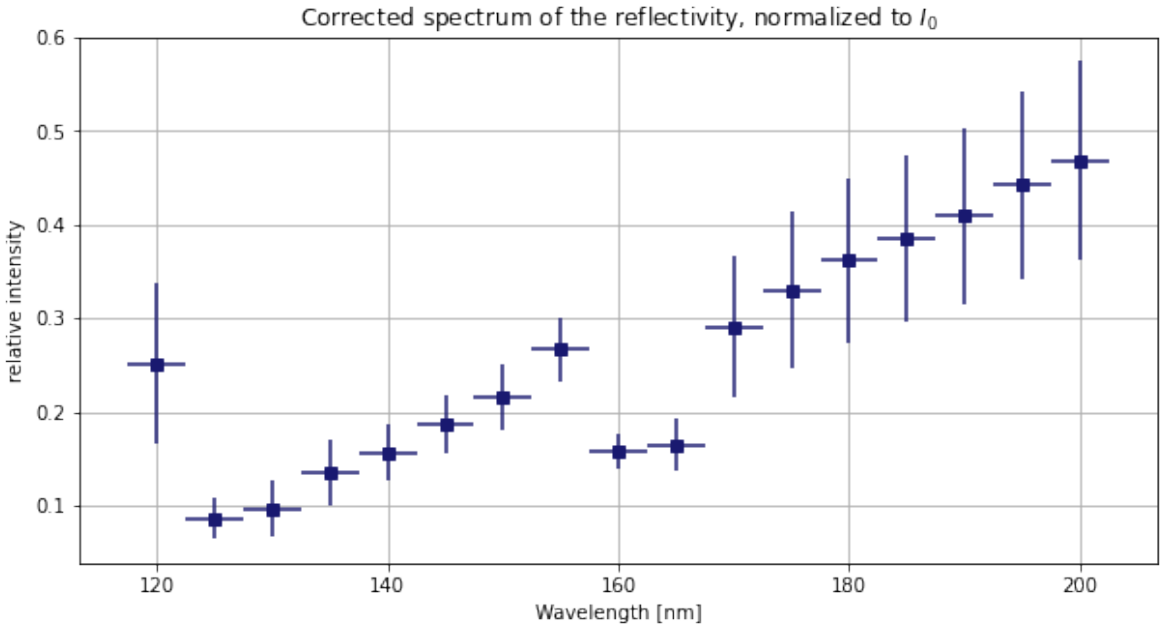

Figure 18: Corrected reflectivity spectrum without the errors of the lamp, grating and SiPM.

References

[1] S. Ahn, *et al.*, Detection of accelerator-produced neutrinos at a distance of 250 km, *Physics Letters B* **511**, 178 (2001).

[2] F. Reines, C. L. COWANjun, The neutrino, *Nature* **178**, 446 (1956).

[3] R. G. Arns, Detecting the neutrino, *Physics in Perspective* **3**, 314 (2001).

[4] R. Davis Jr, D. S. Harmer, K. C. Hoffman, Search for neutrinos from the sun, *Physical Review Letters* **20**, 1205 (1968).

[5] Y. Fukuda, *et al.*, Evidence for oscillation of atmospheric neutrinos, *Physical review letters* **81**, 1562 (1998).

[6] J. W. Valle, Neutrino physics overview **53**, 473 (2006).

[7] B. Abi, *et al.*, The dune far detector interim design report volume 1: physics, technology and strategies, *arXiv preprint arXiv:1807.10334* (2018).

[8] McPHERSON, Vacuum monochromator.

[9] D. R. Paschotta, Rp photonics.

[10] H. Photonics, Tls1017e deuterium lamps (2021).

[11] Nikhef, Detailed setup (2023).

[12] C. van der Post, Vacuum chamber (2022).

[13] S. Gundacker, A. Heering, The silicon photomultiplier: fundamentals and applications of a modern solid-state photon detector, *Physics in Medicine & Biology* **65**, 17TR01 (2020).

[14] Hamamatsu, Sipm model.

[15] O. Stenzel, *et al.*, A model surface for calculating the reflectance of smooth and rough aluminum layers in the vacuum ultraviolet spectral range, *Coatings* **13**, 122 (2023).